WS10-A03

Alternative Multicomponent Observables for Robust Full-waveform Inversion - Application to a Near-surface Example

R. Valensi* (formerly IFSTTAR), R. Brossier (Univ. Grenoble Alpes), D. Leparoux (IFSTTAR) & P. Côte (IFSTTAR)

SUMMARY

In this study, using the framework of the Full Waveform Inversion (FWI) method we compare three different multicomponent cost-functions : the conventional multicomponent cost-function, a cost-function based on the normalized particle motion and a cost function only sensitive to the particle motion polarization.
With a synthetic test, it is showed that even if the attenuation model is poorly estimated the normalized particle motion misfit function and the polarization based cost functions are able to accurately recover the shear wave velocity parameters whereas the conventional multicomponent misfit function fails.
Furthermore in context of near surface imaging, the proposed polarization based cost-function has the advantage to have a great sensitivity to the near-surface and to be independent of the knowledge of the source wavelet.

Introduction

In order to apply the Full Waveform Inversion (FWI) method (Tarantola, 1986; Virieux and Operto, 2009) to near-surface configurations, geophysicists have to consider specific difficulties. Indeed in typical P-SV near-surface configuration, surface waves encode useful information about the subsurface parameters. Even if the shear wave velocity parameters have a dominant impact on the surface waves, when using conventional FWI methods (Pratt and Worthington, 1990) is often preferable to invert simultaneously the V_P parameter (or another elastic parameter providing an equivalent parametrization). However, it has been shown in a context of body-wave inversion that simultaneous inversion of elastic parameters is still challenging (Operto et al., 2013) and it is preferable to employ multicomponent measurements and to include *a-priori* information. In context of near surface imaging, the imaged media can also exhibit a very strong attenuation as well as density heterogeneities (for instance in unconsolidated top layers). The inversion of the attenuation parameters is difficult because of the trade-off between the real and the imaginary part of the velocity parameter (Mulder and Hak, 2009), the need to accurate reproduce amplitude observables and the trade-off with the wavelet inversion (Groos et al., 2014).

As for the deep imaging, the source wavelet is often poorly known, for that reason Pratt and Worthington (1990) proposed to estimate it before inverting structural parameters. However, a successful wavelet inversion with the conventional full-waveform inversion relies on the knowledge of a "good" starting model.

Since the multicomponent measurements are more and more commonly used, vectorial data open perspectives to gain supplementary information. In this communication, we propose to compare the robustness of different misfit functions when decomposing the vectorial measurements in a hierarchical way. The particle motion polarization observables presents interesting properties to deal with the aforementioned difficulties since these observables are independent to the knowledge of the source wavelet and according to Boore and Nafi Toksoz (1969), the polarization has a lower sensitivity to attenuation parameters than for other structural parameters (as for instance velocities) which may prevent the estimation/inversion of the attenuation parameters. Furthermore, in context of near surface imaging the polarization is an observable of choice since Boore and Nafi Toksoz (1969) showed that the polarization can have a great sensitivity to the shallow structures.

Polar decomposition of multicomponent data in the frequency domain and objective functions for vectorial measurements

We consider in the frequency domain a multicomponent field (as for instance the particle velocities, displacements...) composed of only 2 components (P-SV configuration). We can express the particle motion at one location $\mathbf{u}$ according to its polar form : $\mathbf{u} = A_u \mathbf{p}_{u,\phi} e^{\mathrm{i}\phi}$ where A_u is the absolute amplitude (positive real number), $\mathbf{p}_{u,\phi}$ a unit complex vector ($\langle \mathbf{p}_{u,\phi} | \mathbf{p}_{u,\phi} \rangle = 1$) always defined up to a multiplicative constant and $\phi \in [0, 2\pi[$ is the "global" phase. It is noteworthy that the vectors $\mathbf{p}_{u,\phi}$ are equivalent up to a complex phase term. Considering for a given source/receiver couple indexed j,k, the computed $\mathbf{u}^{j,k}_{model}(\mathbf{m}, i_\omega)$ and the observed $\mathbf{u}^{j,k}_{obs}(i_\omega)$ multicomponent observables at the i_ω indexed frequency, we can express the conventional multicomponent FWI misfit function $\mathscr{E}_{conv}(\mathbf{m})$ as :

$$\mathscr{E}_{conv}(\mathbf{m}) = \sum_{i_\omega=1}^{\text{nb frq}} \sum_{j=1}^{\text{nb src}} \sum_{k=1}^{\text{nb rec}} \langle \mathbf{u}^{j,k}_{model}(\mathbf{m}, i_\omega) - \mathbf{u}^{j,k}_{obs}(i_\omega) | \mathbf{u}^{j,k}_{model}(\mathbf{m}, i_\omega) - \mathbf{u}^{j,k}_{obs}(i_\omega) \rangle \tag{1}$$

The cost function $\mathscr{E}_{conv}(\mathbf{m})$ accounts for global amplitudes, global phase and polarization.

When normalizing multicomponent data with the amplitude of the total particle displacement (in order to conserve the polarization) we obtain a cost-function $\mathscr{E}_{norm}(\mathbf{m})$ which is sensitive to the global phase

and the particle motion polarization :

$$\mathscr{E}_{norm}(\mathbf{m}) = \sum_{i_\omega=1}^{\text{nb frq}} \sum_{j=1}^{\text{nb src}} \sum_{k=1}^{\text{nb rec}} \langle \frac{\mathbf{u}^{j,k}_{model}(\mathbf{m}, i_\omega)}{||\mathbf{u}^{j,k}_{model}(\mathbf{m}, i_\omega)||} - \frac{\mathbf{u}^{j,k}_{obs}(i_\omega)}{||\mathbf{u}^{j,k}_{obs}(i_\omega)||} | \frac{\mathbf{u}^{j,k}_{model}(\mathbf{m}, i_\omega)}{||\mathbf{u}^{j,k}_{model}(\mathbf{m}, i_\omega)||} - \frac{\mathbf{u}^{j,k}_{obs}(i_\omega)}{||\mathbf{u}^{j,k}_{obs}(i_\omega)||} \rangle \quad (2)$$

The cost-function $\mathscr{E}_{polar}(\mathbf{m})$ based on the "Poincaré distance" which has been developed by Valensi et al. (2015) is only sensitive to the particle motion polarization :

$$\mathscr{E}_{polar}(\mathbf{m}) = \sum_{i_\omega=1}^{\text{nb frq}} \sum_{j=1}^{\text{nb src}} \sum_{k=1}^{\text{nb rec}} \left(\arccos \left(\left(\frac{2 \left| \langle \mathbf{u}^{j,k}_{obs}(i_\omega) | \mathbf{u}^{j,k}_{model}(\mathbf{m}, i_\omega) \rangle \right|^2}{\langle \mathbf{u}^{j,k}_{model}(\mathbf{m}, i_\omega) | \mathbf{u}^{j,k}_{model}(\mathbf{m}, i_\omega) \rangle \langle \mathbf{u}^{j,k}_{obs}(i_\omega) | \mathbf{u}^{j,k}_{obs}(i_\omega) \rangle} - 1 \right) \right) \right)^2 \quad (3)$$

Implementation in a FWI method code and numerical experiment configuration

The new developments have been implemented in a FWI code developed by Brossier (2011). For the alternative cost-functions (eq. 3 and eq. 2), the main modifications of the inversion code consist in changing the adjoint sources used for the computation of the gradient (adjoint state formalism). The minimization process is based on the computed gradients and the Hessian effect is approximated using a l-BFGS algorithm. When using the cost-functions $\mathscr{E}_{conv}(\mathbf{m})$ and $\mathscr{E}_{polar}(\mathbf{m})$ the source wavelet is inverted following the approach of Pratt and Worthington (1990) whereas with the cost-function $\mathscr{E}_{polar}(\mathbf{m})$ there is no need for source wavelet estimation.

The two main goals of the presented numerical experiment are : first to analyze the effect of reducing the multicomponent information content on the inverted V_S parameter (from the whole multicomponent waveform information with the cost-function $\mathscr{E}_{conv}(\mathbf{m})$ to only the particle motion polarization with the cost function $\mathscr{E}_{polar}(\mathbf{m})$). Second to evaluate the robustness of the presented multicomponent cost-functions to a wrong (overestimation) *a-priori* model of the attenuation parameters.

The numerical experiment consists in inverting simultaneously the V_p and V_s parameters for the model presented in figure 1. In order to estimate the resolution of the reconstruction, we added to V_P and V_S parameters small checkerboard shaped variations with characteristic sizes corresponding to half of the dominant wavelength (Fig. 1). Both compressive and shear waves quality factors (Q_P and Q_S) values are 50 and the density is uniform with a value of 1700 kg/m^3. The imaged media is 126m long and the acquisition is composed of 65 sources and 65 multicomponent receivers (inter-sources and inter-receivers spacing of 2m). The source signal is a Ricker wavelet with a central frequency of 100 Hz. This seismic configuration has been design for reduced scale modeling purposes. However, one can notice that if a scaling factor of 0.5 is applied both on frequencies and on velocities, the configuration get closer to a near surface configurations. The selection of the frequencies has been done according to a Bunks' approach (Bunks et al., 1995) with 6 frequency groups (table 1).

Frequency groups	Frequency content (Hz)
1	50
2	50, 70
3	50, 70, 101
4	50, 70, 101, 129
5	50, 70, 101, 129 , 164,
6	50, 70, 101, 129 , 164, 201

Table 1 *Frequency groups used for the inversion*

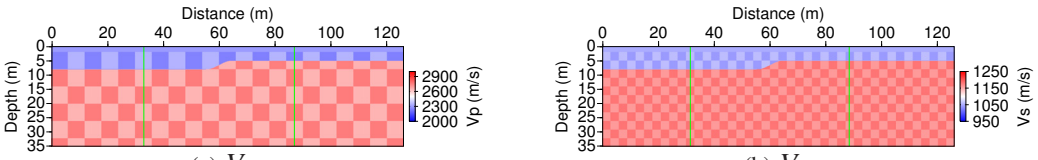

(a) Vp (b) Vs

Figure 1 *: "True" Vp and Vs parameters for the inversion with synthetic data*

Numerical test : inversion results without bias

The inverted results are depicted in figure 2. Even if the V_P and the V_S parameters have been simultaneously inverted, we will only present the results of the V_S parameter. When qualitatively analyzing the figures 2-a,b,c, the inversion results provided by the different cost-functions are quite comparable : the main features of the velocity model are accurately recovered as well as the imprint of the checkerboard is visible. However, we can see that the reconstruction of the checkerboard is slightly better in case of the cost-function $\mathscr{E}_{conv}(\mathbf{m})$ and that the depth of investigation provided by the cost-function $\mathscr{E}_{conv}(\mathbf{m})$ seems to be larger. The velocity logs (Fig. 2-d to 2-i) corroborate the accuracy of the reconstructed models but it can be noticed that only the results obtained with the $\mathscr{E}_{conv}(\mathbf{m})$ misfit function are quantitatively following the slight variations of the true model (Fig. 2-d,c). Also, the results obtained with the polarization only misfit function $\mathscr{E}_{polar}(\mathbf{m})$ exhibit the most accurate reconstructed values of the top layer (from 8m depth on the left-hand side to 5m depth on the right-hand side).

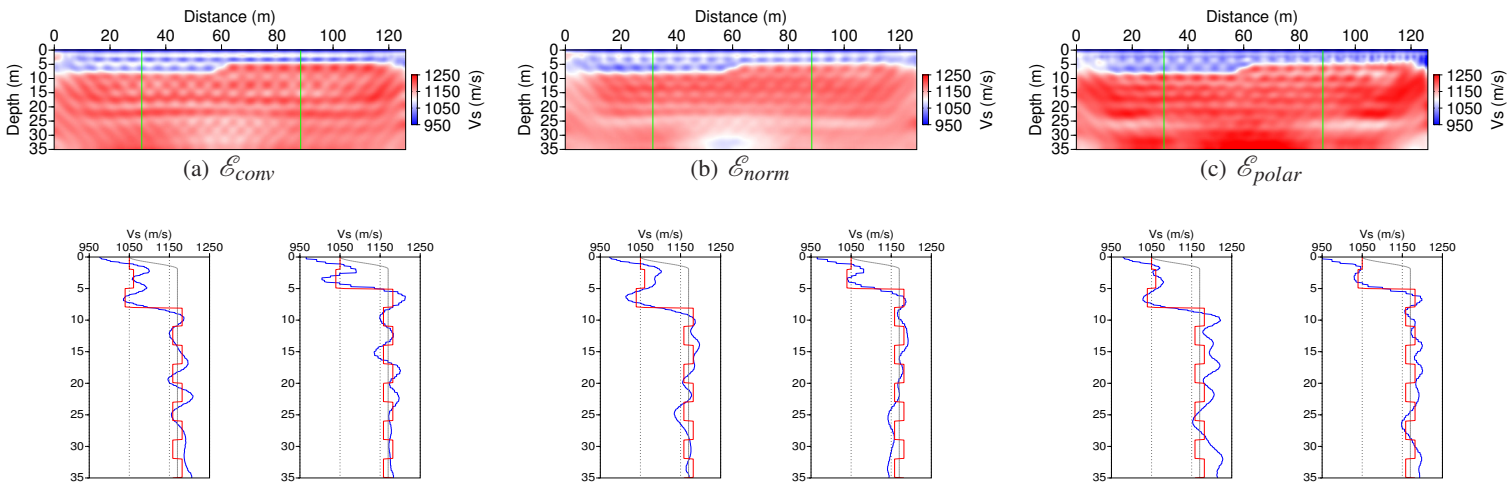

(a) $\mathscr{E}_{conv}$ (b) $\mathscr{E}_{norm}$ (c) $\mathscr{E}_{polar}$

(d) left-hand log (e) right-hand log (f) left-hand log (g) right-hand log (h) left-hand log (i) right-hand log

Figure 2 *: Inversion results of the V_s parameters obtained with the different cost functions without bias. Velocity logs along the vertical lines of the velocity maps are displayed in figures 2-d to 2-f. In the velocity logs, the blue curves represent the inverted values, the red curves the true parameters, and the grey curves the initial model values.*

Numerical test : inversion results with a bias in the *a priori* attenuation model

In order to evaluate the robustness of the different cost functions to bias in the attenuation model, we generate synthetic data with a quality factors $Q_P = Q_S = 20$ and during the whole inversion process it is assumed that $Q_P = Q_S = 50$. The other parameters are strictly the same as in the previous example. Inversion results for the different misfit functions are depicted in figure 3. Clearly, the inversion fails when using the cost-function $\mathscr{E}_{conv}(\mathbf{m})$ (Fig. 3-a,d,e) whereas the inversion results provided by the cost-functions $\mathscr{E}_{norm}(\mathbf{m})$ and $\mathscr{E}_{polar}(\mathbf{m})$ remain comparable to those without bias in the attenuation factor *a priori* model, meaning that with these cost-functions the V_S velocity model is accurately reconstructed.

Conclusions

In this paper, an original way to decompose multicomponent data information in the FWI method has been shown. On a numerical example, it has been shown that the polarization only misfit function is able to recover the velocity parameters of a near-surface model (especially the shallowest part of the

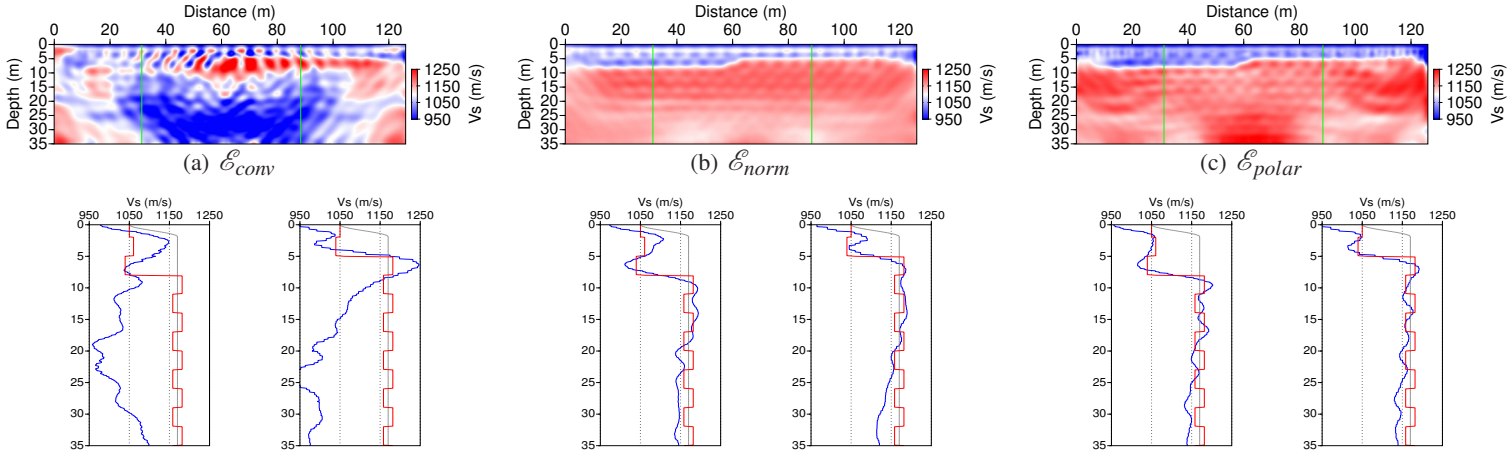

(a) $\mathcal{E}_{conv}$ (b) $\mathcal{E}_{norm}$ (c) $\mathcal{E}_{polar}$

(d) left-hand log (e) right-hand log (f) left-hand log (g) right-hand log (h) left-hand log (i) right-hand log

Figure 3 *: Inversion results of the V_s parameters obtained with the different cost functions with an over-estimation of the quality factors.Velocity logs along the vertical lines of the velocity maps are displayed in figures 2-d to 2-f. In the velocity logs, the blue curves represent the inverted values, the red curves the true parameters, and the grey curves the initial model values.*

model) and it is robust to an overesare timation of the quality factors. Comparable performances are also noticed when the wavefield is normalized by the total particle displacement whereas the effect of errors in estimations of quality factors can be very detrimental when using the whole wavefield (due to the fact that amplitude observables are much more sensitive to attenuation parameters than global phase or polarization observables). Furthermore the polarization observables present other advantages as for instance their insensitivity to the knowledge of the source wavelet or the fact that they are not directly sensitive to kinematic cycle skipping effects.

Acknowledgements

Insightful discussions with Jean Virieux are acknowledged. This work was granted access to the HPC resources of [CINES] under the allocation 2013-[C2013046837] made by GENCI.

References

Boore, D.M. and Nafi Toksoz, M. [1969] Rayleigh wave particle motion and crustal structure. *Bulletin of the Seismological Society of America*, **59**(1), 331–346.

Brossier, R. [2011] Two-dimensional frequency-domain visco-elastic full waveform inversion: Parallel algorithms, optimization and performance. *Computers & Geosciences*, **37**(4), 444 – 455, ISSN 0098-3004, doi:10.1016/j.cageo.2010.09.013.

Bunks, C., Saleck, F.M., Zaleski, S. and Chavent, G. [1995] Multiscale seismic waveform inversion. *GEOPHYSICS*, **60**(5), 1457–1473, doi:10.1190/1.1443880.

Groos, L., Schäfer, M., Forbriger, T. and Bohlen, T. [2014] The role of attenuation in 2d full-waveform inversion of shallow-seismic body and rayleigh waves. *GEOPHYSICS*, **79**(6), R247–R261, doi:10.1190/geo2013-0462.1.

Mulder, W.A. and Hak, B. [2009] An ambiguity in attenuation scattering imaging. *Geophysical Journal International*, **178**(3), 1614–1624, ISSN 1365-246X, doi:10.1111/j.1365-246X.2009.04253.x.

Operto, S. et al. [2013] A guided tour of multiparameter full-waveform inversion with multicomponent data: From theory to practice. *The Leading Edge*, **32**(9), 1040–1054, doi:10.1190/tle32091040.1.

Pratt, R.G. and Worthington, M.H. [1990] Inverse theory applied to multi-source cross-hole tomography. part 1: Acoustic wave-equation method. *Geophysical Prospecting*, **38**, 287–310.

Tarantola, A. [1986] A strategy for nonlinear elastic inversion of seismic reflection data. *Geophysics*, **51**, 1893–1903.

Valensi, R., Brossier, R., Baltazart, V., Leparoux, D., Bretaudeau, F. and Cote, P. [2015] A new kind of polarization-based misfit function: Theoretical formulation and application to full waveform inversion. *77th EAGE Conference & Exhibition 2015, Madrid.*

Virieux, J. and Operto, S. [2009] An overview of full-waveform inversion in exploration geophysics. *Geophysics*, **74**(6), WCC127–WCC152.